IEICE Proceeding Series

# Almost Super Stable Periodic Orbit in an Electric Impact Oscillator

Hiroyuki Asahara, Jun Hosokawa, Kazuyuki Aihara, Soumitro Banerjee, Takuji Kousaka

Vol. 1 pp. 832-835
Publication Date: 2014/03/17
Online ISSN: 2188-5079

2012 International Symposium on Nonlinear Theory and its Applications
NOLTA2012, Palma, Majorca, Spain, October 22-26, 2012

# Almost Super Stable Periodic Orbit in an Electric Impact Oscillator

Hiroyuki Asahara†, Jun Hosokawa†, Kazuyuki Aihara‡, Soumitro Banerjee* and Takuji Kousaka†

† Department of Mechanical and Energy Systems Engineering, Oita University
700 Dannoharu, Oita-shi, Oita, 870-1192 Japan
‡ Institute of Industrial Science, The University of Tokyo
4-6-1 Komaba, Meguro-ku, Tokyo 153-8505, Japan
∗ Indian Institute of Science Education and Research,
West Bengal, Mohanpur, 741252, India
Email: asahara@bifurcation.jp, jun@bifurcation.jp, aihara@sat.t.u-tokyo.ac.jp,
soumitro.banerjee@gmail.com, takuji@oita-u.ac.jp

**Abstract**—In this study, we discuss appearance of an almost super stable periodic orbit (ASSPO) in an electric impact oscillator. First, we show the circuit model and then we explain its dynamics. Next, we derive the Poincaré map and the bifurcation diagram. Finally, we mathematically show appearance of ASSPO through the stability analysis. We believe that appearance of ASSPO is an interesting phenomenon itself because it is a new phenomenon and may also be observed in the other impact oscillators.

## 1. Introduction

The switched dynamical system (SDS) has the interrupted characteristics. We know that there are various kinds of the SDSs in the engineering field. The interrupted or impact systems are the typical example of them. The interrupted system has two or more subsystems that can be interfaced by the switching devices. On the other hand, the impact systems have a discontinuity in the orbit, i.e., the orbit instantly jumps one to the other via the impact. It is important to study the qualitative property of these SDSs not only for the fundamental research but also for the practical application. The bifurcation analysis is one of an effective approach for understanding the qualitative property of the SDSs. There are many papers which have studied the bifurcation phenomena in the SDS, e.g., Refs [1, 2] have studied the switching regulators, and Refs [3, 4, 5] have studied the mechanical impact systems, and so on.

The bouncing ball model is well-known impact system in the mechanical engineering field [6]. The dynamic behavior of it is very simple: a ball bounds on a periodically vibrating table. In spite of that, the bouncing ball model simulates various kinds of the mechanical impact oscillators. For example, the dynamic behavior of the overhead-wire pantograph system of the electric rail way is similar to that of the bouncing ball model [7]. Thus, it is important to study the bouncing ball model, because it is available for understanding the qualitative property of this class of the impact oscillators. The dynamic behavior of it has been intensively studied in the previous works [8, 9, 10]. Moreover, an electrical bouncing ball model has been proposed in Ref. [11]. The electrical model has an advantage in the laboratory experiment and the dynamic behavior of the model is similar to the mechanical bouncing ball closely. Thus, it is also valuable to analyze the electrical bouncing ball model in order to essentially understanding the characteristics of the impact systems. There are some papers which have investigated the nonlinear phenomena in the model. But, all of these papers studied the circuit's dynamics around the period-doubling bifurcation [12, 13]. We know that the electrical bouncing ball has rich interesting nonlinear dynamics other than the period-doubling bifurcation.

In this study, we introduce appearance of the almost super stable periodic orbit (ASSPO) in an electrical bouncing ball. It is an interesting phenomenon itself because there is no study which has investigated the ASSPO in the impact oscillator. First, we show the circuit model [11], and then we explain behavior of the waveform. Next, we derive the Poincaré map and the bifurcation diagram. Using the bifurcation diagram, we show the typical examples of the orbit. Finally, we analyze the stability of the orbit and show that appearance of the ASSPO.

## 2. An electric impact oscillator

Figure 1 shows the circuit model [11]. Basically, the circuit consists of the operational amplifiers: IC1 and IC2 are the integrators, and IC3 is the unity gain adder. The capacitance voltages $v_1$, $v_2$, and an external input voltage $S(t) = v_t \cos \Omega t$ correspond to the ball's position, ball's velocity, and table's position in the mechanical bouncing ball model. In this study, we use the inverting amplifier for $v_1$. The circuit parameters are follows:

$$E_1 = E_2 = 1.5[\mathrm{V}], \quad R_1 = 1.0[\mathrm{M\Omega}], \quad R_2 = R_3 = 10[\mathrm{k\Omega}],$$
$$R_f = 2.0[\mathrm{M\Omega}], \quad C_1 = 33.0[n\mathrm{F}], \quad C_2 = C_f = 0.1[\mu\mathrm{F}]. \tag{1}$$

The circuit equation is given by

$$\begin{cases} \dfrac{dv_1}{dt} = -\dfrac{1}{R_2C_2}v_2 \\ \dfrac{dv_2}{dt} = i_d(v_3) + \dfrac{1}{R_1C_1}E \end{cases}. \tag{2}$$

$i_d(v_3)$ and $v_3$ are defined as follows:

$$i_d(v_3) = \begin{cases} -\dfrac{1}{R_fC_1}v_3 - \dfrac{C_f}{C_1}\dfrac{dv_3}{dt}, & v_3 > 0 \\ 0, & v_3 \le 0 \end{cases}, \tag{3}$$

where $v_3$ is

$$v_3 = -v_2 - S(t). \tag{4}$$

We use the following values:

$$x = v_1, \quad y = v_2, \quad z = v_3, \quad a = v_t, \quad \omega = \Omega R_2C_2,$$
$$\tau = \frac{t}{R_2C_2}, \quad \alpha = \frac{R_2C_2}{R_fC_1}, \quad \beta = \frac{C_f}{C_1}, \quad \gamma = \frac{R_2C_2}{R_1C_1}E. \tag{5}$$

Thus, Eq. (2) is rewritten as follows:

$$\begin{array}{ll} \dot{\boldsymbol{u}} = \boldsymbol{A}_1\boldsymbol{u} + \boldsymbol{B}_1, & \text{Diode: ON} \\ \dot{\boldsymbol{u}} = \boldsymbol{A}_2\boldsymbol{u} + \boldsymbol{B}_2, & \text{Diode: OFF} \end{array}, \tag{6}$$

where $\boldsymbol{u} = (x, y)^\top$, $\top$ denotes transpose. $\boldsymbol{A}_i$ and $\boldsymbol{B}_i$ $(i = 1, 2)$ are defined as follows:

$$\boldsymbol{A}_1 = \begin{bmatrix} 0 & -1 \\ 0 & 0 \end{bmatrix}, \boldsymbol{A}_2 = \begin{bmatrix} 0 & -1 \\ \alpha & -\beta \end{bmatrix}, \tag{7}$$

$$\boldsymbol{B}_1 = \begin{bmatrix} 0 \\ 0 \end{bmatrix}, \boldsymbol{B}_2 = \begin{bmatrix} 0 \\ \alpha a\cos(\omega\tau) - \beta a\omega\sin(\omega\tau) + \gamma \end{bmatrix}. \tag{8}$$

The external input is given by

$$S(\tau) = a\cos\omega\tau. \tag{9}$$

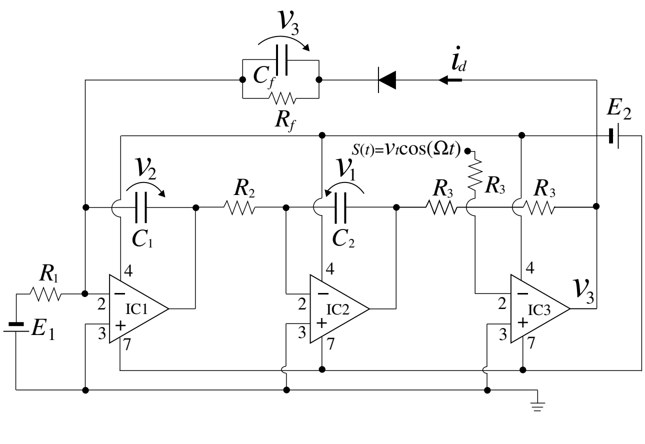


Figure 1: Circuit model.

The switching condition $z$ is defined as

$$z = -x - S(\tau), \tag{10}$$

where the diode is opened if $z > 0$, otherwise the diode is closed. The parameters $\alpha$, $\beta$ and $\gamma$ are fixed as $\alpha = 15.0$, $\beta = 3.0$ and $\gamma = 0.05$ in the following analysis.

Figure 2 shows a typical example of the waveforms in the circuit. The red-colored waveform $x(\tau)$ denotes the displacement of the ball, the green-colored waveform $y(\tau)$ denotes the velocity of the ball, and yellow-colored waveform $S(\tau)$ denotes the displacement of the table, respectively. When $x(\tau)$ hits the $S(\tau)$, i.e., $x(\tau) \le S(\tau)$, the diode changes from closed to opened. After that, the diode changes from opened to closed again if $x(\tau) > S(\tau)$ is satisfied.

## 3. Analytical results

Figure 3 shows an example of the one-parameter bifurcation diagram. The bifurcation parameter $\omega$ is increased from $\omega = 0.4$ to $\omega = 0.7$ and we show a part of the one-parameter bifurcation diagram. The $y$-axis $x_k$ denotes a sampled data: we sampled the waveform $x(\tau)$ at every period of $T$ (see the blue points in Fig. 2).

The circuit has rich interesting phenomena, but we only focus on the period-3 orbit in the following analysis. Figure 4 shows the period-3 orbits. It is clear from Fig. 4 that these period-3 orbits are different types of the period-3 orbit, because the mapping points are not same (see the blue-colored mapping points). However, we find that a part of the mapping point is certainly on $(x, y) = (-0.4, 0.0)$ (see the mapping point in red-colored area). In this situation, the value of the waveform $x(kT)$ is very close to that of $S(kT)$, i.e., the waveform $x(\tau)$ is almost slipping on the waveform $S(\tau)$ around $\tau = kT$. Thus, we can understand that why these period-3 orbits have a mapping point on $(x, y) = (-0.4, 0.0)$; because $x(kT) = S(kT) = -0.4$ and $y(kT) = \frac{dS(\tau)}{d\tau}\Big|_{\tau=kT} = 0.0$.

At the next stage, we mathematically investigate the mechanism of the period-3 orbit corresponding to (a) in Fig. 4 as an example. Generally, we have to calculate the

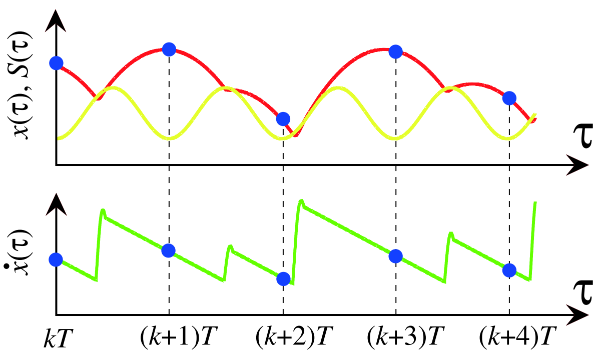


Figure 2: Example of the waveforms.

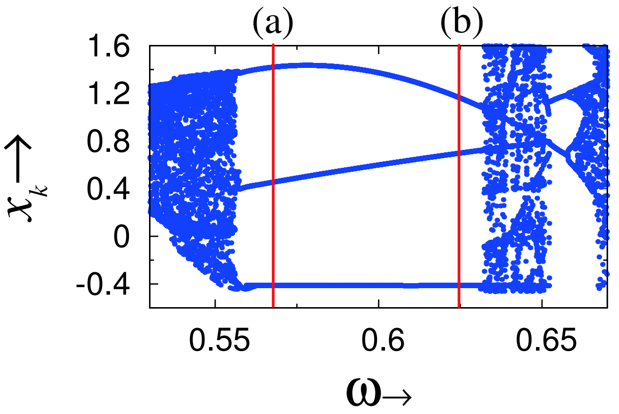


Figure 3: An example of the one-parameter bifurcation diagram.

characteristic multiplier of the orbit for understanding the characteristics of the above period-3 orbit. Here, we use the method reported in [14] for the stability analysis. Figure 5 shows an example of the enlarged waveform of the period-3 orbit corresponding to Fig. 4 (a). Based on the figure, we derive the characteristic multipliers of the period-3 orbit. The Jacobian matrix $\boldsymbol{M}$ is defined as follows:

$$\boldsymbol{M} = \boldsymbol{M}_1 \cdot \boldsymbol{M}_2 \cdot \boldsymbol{M}_3, \tag{11}$$

where, $\boldsymbol{M}_1$, $\boldsymbol{M}_2$, and $\boldsymbol{M}_3$ are given by

$$\boldsymbol{M}_1 = e^{\mathbf{A}_1\tau_9} \cdot \mathbf{S}_{\text{off}}(2T+\tau_8) \cdot e^{\mathbf{A}_2\tau_8} \mathbf{S}_{\text{on}}(2T+\tau_7) \cdot e^{\mathbf{A}_2\tau_7}, \tag{12}$$

$$\boldsymbol{M}_2 = \cdot e^{\mathbf{A}_1\tau_6} \cdot \mathbf{S}_{\text{off}}(2T-\tau_6) \cdot e^{\mathbf{A}_2\tau_5} \cdot \mathbf{S}_{\text{on}}(T+\tau_4) \cdot e^{\mathbf{A}_1\tau_4}, \tag{13}$$

$$\boldsymbol{M}_3 = e^{\mathbf{A}_1\tau_3} \cdot \mathbf{S}_{\text{off}}(\tau_1+\tau_2) \cdot e^{\mathbf{A}_2\tau_2} \cdot \mathbf{S}_{\text{on}}(\tau_1) \cdot e^{\mathbf{A}_1\tau_1}. \tag{14}$$

$\boldsymbol{A}_1$ and $\boldsymbol{A}_2$ denote the subsystem matrix (see Eq. (7)). Times $\tau_1$, $\tau_2$, $\tau_3$, $\tau_4$, $\tau_5$, $\tau_6$, $\tau_7$, $\tau_8$, and $\tau_9$ are drown in Fig. 5. The state transition matrix $\boldsymbol{S}_{\text{on}}(\tau)$ and $\boldsymbol{S}_{\text{off}}(\tau)$ are defined as follows:

$$\boldsymbol{S}_{\text{on}}(\tau) = \begin{bmatrix} 1 & 0 \\ \dfrac{\alpha x(\tau) - \beta y(\tau) + \alpha a \cos(\omega\tau) - \beta a\omega \sin(\omega\tau)}{y(\tau) + a\omega \sin(\omega\tau)} & 1 \end{bmatrix}, \tag{15}$$

$$\boldsymbol{S}_{\text{off}}(\tau) = \begin{bmatrix} 1 & 0 \\ \dfrac{-\alpha x(\tau) + \beta y(\tau) - \alpha a \cos(\omega\tau) + \beta a\omega \sin(\omega\tau)}{y(\tau) + a\omega \sin(\omega\tau)} & 1 \end{bmatrix}. \tag{16}$$

The characteristic multipliers $\mu$ is given by solving the following equation:

$$\det\left[\boldsymbol{M} - \mu\boldsymbol{I}\right] = \boldsymbol{0}, \tag{17}$$

where $\boldsymbol{I}$ denotes the unit matrix. Table 1 shows the characteristic multipliers $\mu$ of the period-3 orbit. The table implies that there is the almost super stable period-3 orbit (ASSPO-3), because the characteristic multipliers satisfies $\mu \approx 0.0$. We consider that the ASSPO appears when the waveform is slipping on the sinusoidal wave.

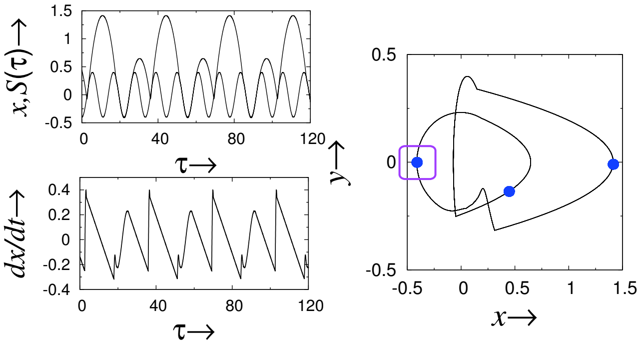


(a) Corresponds to a parameter (a) in Fig. 3

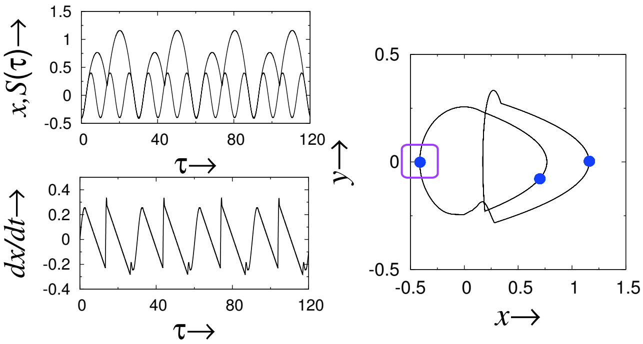


(b) Corresponds to a parameter (b) in Fig. 3

Figure 4: Typical examples of the ASSPO.

Table 1: Characteristic multipliers $\mu_1$ and $\mu_2$ of the period-3 orbit

| $\omega$ | $\mu_1, \mu_2$ | Remark |
|---|---|---|
| 0.557633 | -0.000000, 0.000022 | ASSPO-3 |
| 0.557570 | -0.000000, 0.000022 | ASSPO-3 |
| 0.557507 | -0.000000, 0.000023 | ASSPO-3 |

## 4. Conclusion

In this study, we have confirmed existence of the ASSPO in an electric impact oscillator. First, we showed the circuit model and then we explained behavior of the waveform. Next, we derived the Poincaré map and the bifurcation diagram. Based on the Poincaré map, we visually explained existence of the ASSPO. Finally, we calculated the characteristic multipliers of a ASSPO-3. Appearance of the ASSPO is an interesting phenomenon itself because no paper report such kind of phenomenon in the impact oscillator. We consider that the ASSPO appears when the waveform is slipping on the sinusoidal wave. We know that the slipping phenomenon is also observed in the other impact oscillators, i.e., the overhead-wire pantograph system of the electric rail way. In addition, the circuit dynamics is similar to the overhead-wire pantograph system. Therefore, we consider that the ASSPO will also appear in the

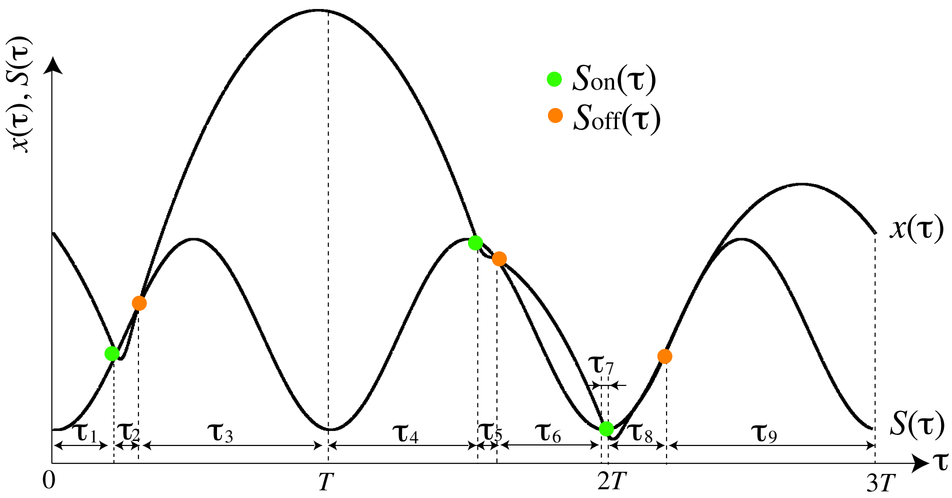


Figure 5: Conceptual diagram for the stability analysis.

overhead-wire pantograph system. We believe that ASSPO has a key to developing the nonlinear theory of the impact oscillators because ASSPO is a new phenomenon and will be observed not only in the electrical bouncing ball model but also in the other impact systems. In future, we will study the bifurcation phenomena around the ASSPO.

## Acknowledgments

This research is partially supported by the Aihara Innovative Mathematical Modelling Project, the Japan Society for the Promotion of Science (JSPS) through the "Funding Program for World-Leading Innovative R & D on Science and Technology (FIRST Program)," initiated by the Council for Science and Technology Policy (CSTP).

## References


[1] S. Banerjee and G.C. Verghese., "Nonlinear Phenomena in Power Electronics: Attractors, Bifurcations, Chaos, and Nonlinear Control," Piscataway, NJ: IEEE Press, 2001.

[2] C.K. Tse., "Complex Behavior of Switching Power Converters," Boca Raton: CRC Press, 2003.

[3] S. Foale and S. R. Bishop., "Bifurcations in impact oscillations," Springer 1994.

[4] M. Bernardo, C.J. Budd, A.R. Champneys, P. Kowalczyk., "Piecewise-smooth Dynamical Systems," Springer 2008.

[5] G. Ikeda, K. Aihara and T. Kousaka, "Calculation Method of Bifurcation Point for an Impact Oscillator with Periodic Function," Proc. CHAOS, 2012. (In press)

[6] N. B. Tufillaro, T. M. Mell, Y. M. Choi and A. M. Albano., "Period doubling boundaries for a bouncing ball," J. Physique, Vol. 47, pp. 1477-1482, 1986.

[7] S. Kawamura, K, Kitajo, S. Horita and M. Yoshizawa., "Fundamental study on impact oscillations of rigid trolley-pantograph system," The Japan Society of Mechanical Engineers C, Vol.73, No. 728, pp. 974-981, 2007. (In Japanese)

[8] S. Giusepponia, F. Marchesonia and M. Borromeob., "Randomness in the bouncing ball dynamics," Physica A, Vol. 351, pp. 142-158, 2005.

[9] C. J. Budd and P. T. Piiroinen., "Corner bifurcations in non-smoothly forced impact oscillators," Physica D, Vol. 220, pp. 127-145, 2006.

[10] A. B. Nordmark and P. T. Piiroinen, "Simulation and stability analysis of impacting systems with complete chattering," Nonlinear Dynamics, Vol. 58, No.1-2, pp. 85-106, 2009.

[11] R. L. Zimmeman, S. Celaschi, "The electronic bouncing ball," Am. J. Phys, Vol. 60, pp. 370-375, 1992.

[12] B. K. Clark, E. Rosa Jr, A. D. Hall, T. R. Shpherd, "Dynamics of an electronic impact oscillator," Phys. Letters, Vol. 318, pp. 514-521, 2003.

[13] J. Hosokawa, H. Asahara, K. Aihara, T. Kousaka, "Bifurcation phenomena in an electric impact oscillator," Proc. ITC-CSCC 2011, pp. 870-873, 2011.

[14] D. Giaouris, S. Banerjee, B. Zahawi, V. Pickert, "Stability Analysis of the Continuous-Conduction-Mode Buck Converter Via Filippov's Method" IEEE Trans. Circ. Syst. I, Vol. 55, No. 4, pp. 1084-1096, 2008.